Solvable model for quantum wavepacket scattering in one dimension

1998 J. Phys. A: Math. Gen. 31 9519

(http://iopscience.iop.org/0305-4470/31/47/012)

J. Phys. A: Math. Gen. **31** (1998) 9519–9534. Printed in the UK PII: S0305-4470(98)93615-0

Solvable model for quantum wavepacket scattering in one dimension

J G Muga† and J P Palao
Departamento de Física Fundamental y Experimental, Universidad de La Laguna, Tenerife, Spain

Received 23 April 1998

Abstract. Quantum wavepacket collisions of a Lorentzian state with a separable potential are described analytically. This model problem illustrates many different aspects of time-dependent scattering: in particular, the effects associated with resonance poles (time delay, exponential decay) and other critical points in the complex momentum plane, the effects of complex absorbing potentials, as well as some unique aspects of short- and long-time behaviour.

1. Introduction

Analytically solvable models are useful research tools to check the validity of hypotheses, new calculation methods, and/or approximations. They also lead occasionally to the discovery of new physical effects. Few models exist that allow an explicit analytical examination of time-dependent scattering. Elberfeld and Kleber described the collision of a wavepacket, initially a Lorentzian-like function in momentum representation, with a delta function potential [1]. The model has found some applications [2], but it is somewhat limited because it does not consider resonances. The first aim of this paper is to provide an analytical description of a wavepacket colliding with a separable potential (real or complex) that admits resonance scattering. Then the model is applied to illustrate a number of propagation characteristics. Some of them are well known but are included for completeness, such as time delays or exponential decay. Others are not: for example, the build-up regime previous to the exponential decay, deformations due to the resonances, very short or very large times, low-energy scattering, interferences between the 'free' and 'scattered' components, the effect of 'spurious' poles and other singularities in the complex momentum plane, or time-dependent scattering of absorptive potentials (where an interesting negative delay phenomenon for the transmitted packet, versus a positive delay for the reflected one, is described).

The stationary and time-dependent regimes are described in sections 2 and 3 respectively. In section 4 the different applications are discussed.

2. Separable potential: stationary scattering

A separable potential model has been used in a number of previous works for different purposes [3–13],

$$V = |\chi\rangle v \langle\chi| \qquad \langle p|\chi\rangle = \left(\frac{2}{\pi}\right)^{1/2} \frac{1}{1+p^2}. \tag{1}$$

† Author to whom correspondence should be addressed. E-mail address: jmuga@ull.es

0305-4470/98/479519+16$19.50

In this work all variables (position, momentum, energy, time) are dimensionless†. Before discussing time-dependent scattering it is useful to first examine the stationary regime. General properties of separable potentials have been examined by Ghirardi and Rimini [14]. For the particular form (1) the stationary scattering has been studied in the unitary case (v real) [3, 5]. Here we shall briefly review the main results, and then extend the analysis to the absorptive case. The S matrix [15] is diagonal for symmetric and antisymmetric combinations of plane waves. Its two elements in this basis are

$$\begin{aligned} S_0 &= \eta_0 e^{2i\delta_0} = T + R = \frac{(p+i)^2 C^*(p^*, v^*)}{(p-i)^2 C(p, v)} \\ S_1 &= \eta_1 e^{2i\delta_1} = T - R = 1 \end{aligned} \tag{2}$$

where

$$C(p, v) \equiv p(p+i)^2 - 2v(p+2i). \tag{3}$$

T and R are transmission and reflection amplitudes, $\eta_{0,1}$ are (real) 'inelasticity parameters' [16], and $\delta_{0,1}$ (real) phase shifts. A peculiarity of this potential is its 'transparency' for antisymmetric waves, $\eta_1 = 1$, $\delta_1 = 0$.

For even potentials the transmission, reflection and absorption coefficients can be written in terms of the phase shifts, see (2), as

$$\mathcal{T} \equiv |T|^2 = \left(\frac{\eta_0 - \eta_1}{2}\right)^2 + \eta_0\eta_1 \cos^2(\delta_0 - \delta_1) \tag{4}$$

$$\mathcal{R} \equiv |R|^2 = \left(\frac{\eta_0 - \eta_1}{2}\right)^2 + \eta_0\eta_1 \sin^2(\delta_0 - \delta_1) \tag{5}$$

$$\mathcal{A} \equiv 1 - \mathcal{T} - \mathcal{R} = 1 - \tfrac{1}{2}(\eta_0^2 + \eta_1^2). \tag{6}$$

The maximum absorbance occurs when one of the roots of $C^*(p^*, v^*)$ crosses the real axis so that $S_0 = \eta_0 = 0$.

The roots of $C(p, v)$ will be denoted as p_j, $j = 1, 2, 3$, while the roots of $C^*(p^*, v^*)$ are $-p_j$. The latter are zeros of S_0 and the former are poles. The motion of the roots of $C(p, v)$ due to variations of v was described in [5] for real v. In particular, when $v > (-11 + 5\sqrt{5})/4$, there are two roots with opposite real parts on both sides of the negative imaginary axis, the 'resonance' and 'antiresonance' poles of S_0 (p_1 and p_2 in the fourth and third quadrant respectively), and a third root in the negative imaginary axis (p_3), a 'virtual state pole' that approaches $-2i$ as $v \to \infty$. The resonance pole leads to a peak in the reflection probability for $v > \frac{1}{6}$, or, equivalently, a minimum in the transmission probability (see figure 1). Note also the zero energy minimum related to the combined effect of the virtual pole p_3 and the double 'spurious' pole at $p = i$ [5]. The resonance pole causes, when sufficiently close to the real axis, sudden jumps of the phase shift by approximately π (see figure 2). In general these jumps may lead to a maximum or a minimum of the reflectance depending on the 'background' phase $(\delta_0 - \delta_1)_{bg}$. (The present model provides a maximum while the square barrier is a well known example of minimum reflection at resonance.)

When v is real, for every pole of S_0 at p_j there is a zero Z_j at p_j^*, see (2). The distance from any real p to both points (zero and pole) is equal, so that S_0 factorizes in contributions

† The dimensionless momentum, position and time, are related to the corresponding dimensional quantities, denoted here with a tilde, by the following expressions: $p = \tilde{p}/a$, $x = a\tilde{x}/\hbar$ and $t = \tilde{t}a^2/(m\hbar)$, whereas the potential constants (and similarly all energies) are linked by $v = m\tilde{v}/a^2$. a is the characteristic momentum of the system.

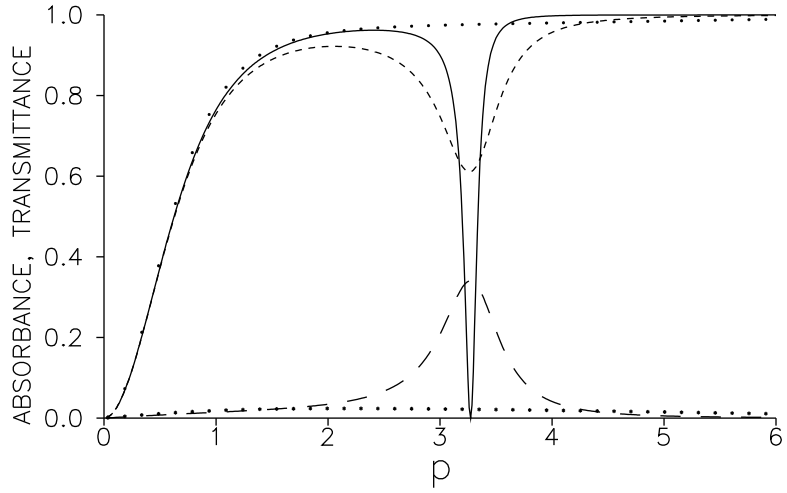

Figure 1. Transmittance and absorbance versus p for $\mathrm{Re}\,(v) = 5$: transmittances for $\mathrm{Im}\,(v) = 0$ (full curve), $\mathrm{Im}\,(v) = -0.8$ (short broken curve), and $\mathrm{Im}\,(v) = -20$ (upper dotted curve). Absorbances for $\mathrm{Im}\,(v) = -0.8$ (long broken curve), and $\mathrm{Im}\,(v) = -20$ (lower dotted curve).

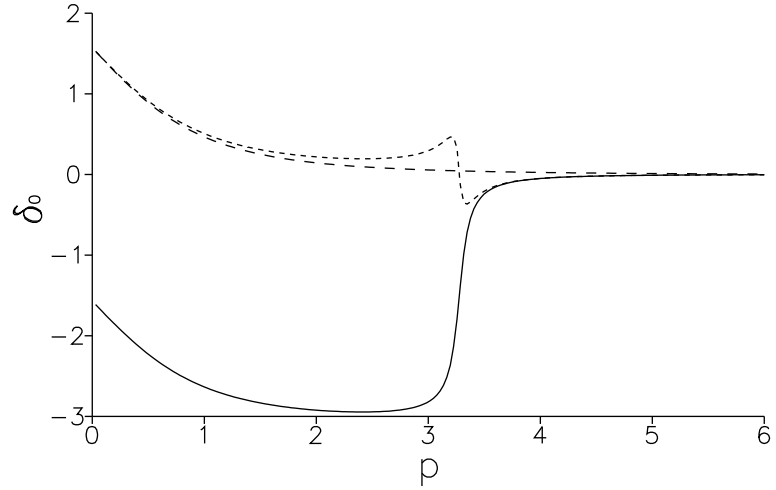

Figure 2. $\delta_0(p)$ versus p for $\mathrm{Re}\,(v) = 5$: $\mathrm{Im}\,(v) = 0$ (full curve), $\mathrm{Im}\,(v) = -0.3$ (short broken curve), and $\mathrm{Im}\,(v) = -20$ (long broken curve).

of unit modulus from each zero-pole pair [5]. However, the addition of an imaginary part to v breaks this symmetry. If the zero Z_j is closer to the real axis than the pole p_j, absorption occurs in the proximity of the pair because $|p - Z_j|/|p - p_j| < 1$. Figure 3 shows the motion of zeros and poles of S_0 when $-\mathrm{Im}\,(v)$ is increased. The resonance zero-pole pair goes down, towards the bisector of the fourth quadrant, and the antiresonance zero-pole pair goes up, towards the bisector of the second quadrant.

When, at a critical value $\mathrm{Im}\,(v) = I_c$, the zero Z_1 associated with the resonance pole crosses the real axis, S_0 vanishes for the real momentum of the zero, and maximum absorption occurs. Simultaneously, the antiresonance pole crosses the real negative axis so that, in accordance with Levinson's theorem [17, 18], there is a discontinuous jump

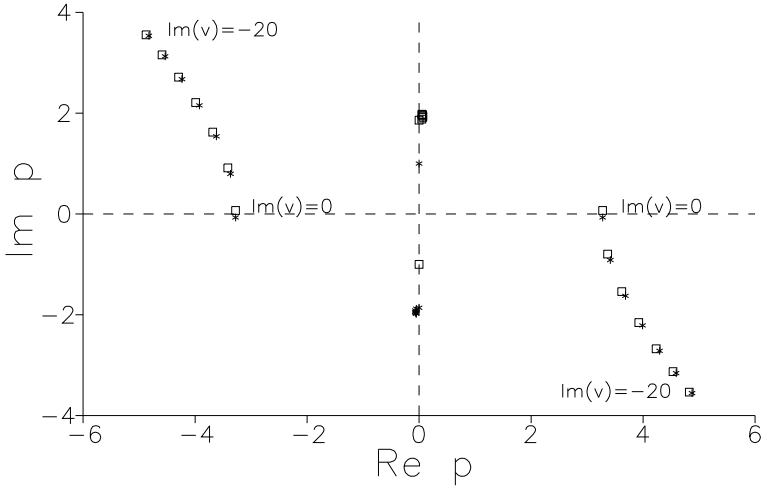

Figure 3. Motion of zeros (squares) and poles (stars) of S_0 in the complex momentum plane p for $\mathrm{Re}\,(v) = 5$, from $\mathrm{Im}\,(v) = 0$ to $\mathrm{Im}\,(v) = -20$.

in the phase shift δ_0 at the origin. (The possible 2π ambiguities in the definition of δ_0 are fixed by imposing $\delta_0(\infty) = 0$ and continuity.) The unusual fact with respect to the unitary case is that this jump is not caused by a new (regular) bound state of real negative energy (represented by a pole in the positive imaginary axis), but by a new 'localized state' represented by a pole in the second quadrant of the momentum plane [17, 19]. It has positive real energy and a negative imaginary energy so that its norm disappears exponentially with time. For $\mathrm{Im}\,(v)$ slightly more negative than I_c the slope of δ_0 is negative at resonance, which physically implies an anomalous negative time delay τ_0,

$$\tau_0 \equiv \frac{2}{p}\frac{\partial \delta}{\partial p} \tag{7}$$

or time advance, instead of the standard (positive) resonance time delay found in the Hermitian case [20].

By decreasing further $\mathrm{Im}\,(v)$ to more negative values the zero-pole pair moves away from the real axis and the resonance width broadens until the peak in the reflectance eventually disappears (see figure 1). For fixed $\mathrm{Re}\,(v)$ the asymptotic behaviour as $\mathrm{Im}\,(v) \to -\infty$ of the roots of $C(p, v)$ is $p_1 \sim [-\mathrm{Im}\,(v)]^{1/2}(1 - \mathrm{i})$, $p_2 \sim [-\mathrm{Im}\,(v)]^{1/2}(\mathrm{i} - 1)$, and $p_3 \sim -2\mathrm{i}$. Since p_1 and the associated zero Z_1 converge, the absorption tends to vanish.

A complementary view of the above discussion is provided by representations of the imaginary part versus the real part of S_0 (Argand diagrams) from a large value of p to $p = 0$, and for different values of $\mathrm{Im}\,(v)$ (see figure 4 and compare with figure 2).

The properties of the elements of the S matrix in the representation of plane waves impinging from one side, namely the reflection and transmission amplitudes, are also of interest since several important features of wave propagation depend directly on them. In particular, the time delays are given by

$$\tau_T = \frac{1}{p}\frac{\partial \phi_T}{\partial p} \qquad \tau_R = \frac{1}{p}\frac{\partial \phi_R}{\partial p} \tag{8}$$

where ϕ_T and ϕ_R are the phases of the transmission and reflection amplitudes ($T = |T|\exp(\mathrm{i}\phi_T)$ and $R = |R|\exp(\mathrm{i}\phi_R)$). For real v it follows from the unitarity of the S

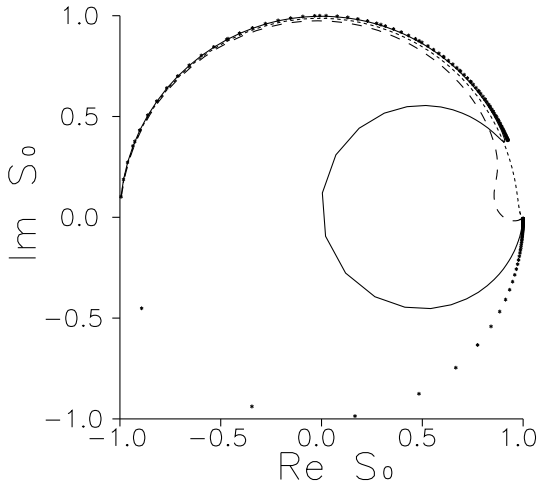

Figure 4. Im (S_0) versus Re (S_0). In all cases Re $(v) = 5$, and Im $(v) = 0$ (dots for equally spaced values of p): Im $(v) = -0.223$ (full curve), Im $(v) = -0.8$ (long broken curve), and Im $(v) = -20$ (short broken curve).

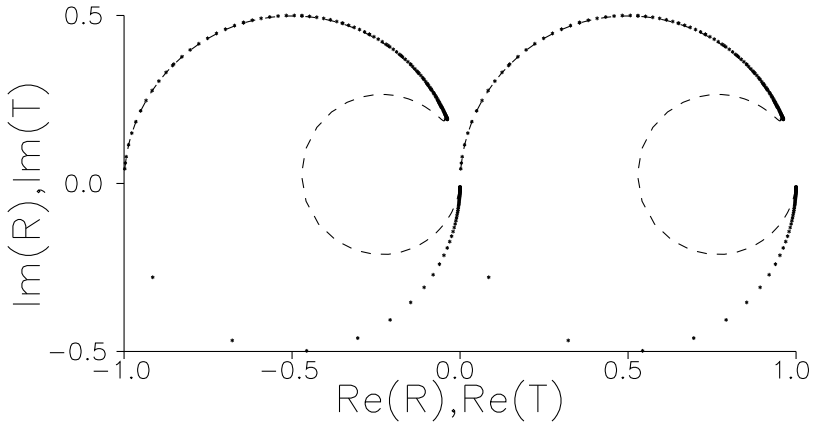

Figure 5. Im (T) versus Re (T) (right curves) and Im (R) versus Re (R) (left curves). Re $(v) = 5.0$: Im $(v) = -0.000\,01$ (dots for equally spaced values of p), and Im $(v) = -0.25$ (broken curve).

matrix that the phases of T and R only differ by an odd multiple of $\pi/2$†, so that the two delays are equal, $\tau_R = \tau_T$. But this is no longer true when an imaginary part is added to the potential. There is a zero of T at resonance for Im $(v) = 0$. For values of Im (v) slightly more negative, this zero moves off the real axis and the derivative of ϕ_T changes sign at resonance. This is similar to the effect discussed before for δ_0. (The difference is that the critical value of Im (v) here is 0 instead of I_c.) In contrast, the phase of R does not suffer any dramatic change (see the Argand diagrams, ϕ_T, and ϕ_R for Im $(v) = -0.000\,01$ and Im $(v) = -0.25$ in figures 5 and 6).

† This relation is obtained from the non-diagonal elements of the matrix equation $SS^{\dagger} = 1$ for even potentials.

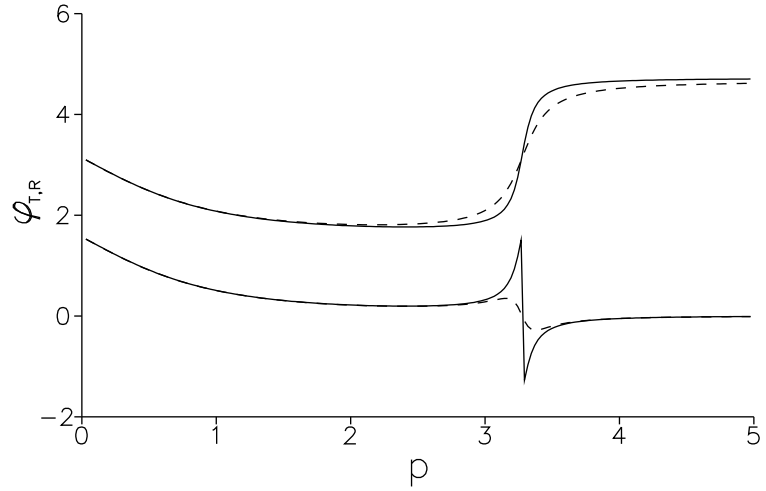

Figure 6. $\phi_T(p)$ (two lower curves) and $\phi_R(p)$ (upper curves), for $\mathrm{Im}\,(v) = -0.000\,01$ (full curve), and -0.25 (broken curve); $\mathrm{Re}\,(v) = 5$.

3. Wavepacket scattering

In order to find an explicit wavefunction in the time dependent case the state at the initial (preparation) time $t = 0$ is chosen as the one considered by Elberfeld and Kleber [1]. In momentum representation it is given by a Lorentzian-type function,

$$\langle p|\mathcal{L}\rangle = \mathrm{e}^{-\mathrm{i}x_c p}\left(\frac{2b^3}{\pi}\right)^{1/2}\frac{1}{b^2+(p-p_c)^2}. \tag{9}$$

b is related to the width of the momentum distribution $|\langle p|\mathcal{L}\rangle|^2$. ($[2^{1/2}-1]^{1/2}b \approx 0.64b$ is the half width at half height.) It is always assumed that $x_c < 0$.

The wavefunction at an arbitrary time $t > 0$ and position x can be obtained by using a contour integral representation of the evolution operator $U(t) \equiv \mathrm{e}^{-\mathrm{i}Ht}$ in the complex momentum q-plane in terms of the resolvent $(z-H)^{-1}$,

$$\langle x|U(t)|\mathcal{L}\rangle = \frac{\mathrm{i}}{2\pi}\int_\Gamma \mathrm{d}q\, q\langle x|\frac{\mathrm{e}^{-\mathrm{i}zt}}{z-H}|\mathcal{L}\rangle \tag{10}$$

where $z = q^2/2$ is the complex energy. The integral contour Γ goes from $-\infty$ to $+\infty$ in the complex momentum q-plane passing above all the singularities of the resolvent in the upper half-q-plane (first energy sheet). For v real these singularities correspond to the discrete bound states of the Hamiltonian on the positive imaginary q-axis and the continuous spectrum on the real axis; for a potential having a negative imaginary part, there may be also an antiresonance pole in the second quadrant.

The resolvent can be separated into 'free motion' and scattering parts,

$$\frac{1}{z-H} = \frac{1}{z-H_0} + \frac{1}{z-H_0}T_{\mathrm{op}}(z)\frac{1}{z-H_0} \tag{11}$$

where the parametrized transition operator $T_{\mathrm{op}}(z)$ has been introduced. Using (1) and (11) one finds the explicit expression

$$T_{\mathrm{op}}(z) = |\chi\rangle\frac{vq(q+\mathrm{i})^2}{C(q)}\langle\chi| \tag{12}$$

where $C(q)$ is the cubic polynomial (3) introduced in the previous section.

The resolvent decomposition leads to a parallel decomposition of the evolution operator into a free motion part, $U_0 = \mathrm{e}^{-\mathrm{i}H_0 t}$, and a scattering part, $U_s = \mathrm{e}^{-\mathrm{i}Ht} - \mathrm{e}^{-\mathrm{i}H_0 t}$. Using (10)–(12) one finds for the free and scattering parts of the wavefunction,

$$\langle x|\psi_{0,s}(t)\rangle = \langle x|U_{0,s}|\mathcal{L}\rangle = \frac{\mathrm{i}}{2\pi}\int \mathrm{d}q\, \mathrm{e}^{-\mathrm{i}zt} I_{0,s}(q) \tag{13}$$

where

$$I_0(q) = \langle x|\frac{q}{z-H_0}|\mathcal{L}\rangle \tag{14}$$

$$I_s(q) = \langle x|\frac{q}{z-H_0}|\chi\rangle \frac{vq(q+\mathrm{i})^2}{C(q)} \langle\chi|\frac{1}{z-H_0}|\mathcal{L}\rangle. \tag{15}$$

The matrix elements involved can be obtained by expanding the free Hamiltonian in momentum eigenfunctions and using contour integration. Inserting them into the integrals (13) the scattering part is decomposed into six terms denoted as ψ_n, $n = 1, \ldots, 6$, and the free part provides a term ψ_0. All of them can be expressed in the general form

$$\psi_n = K_n \int_\Gamma \mathrm{d}q\, R_n(q) \mathrm{e}^{-\mathrm{i}zt} \mathrm{e}^{-\mathrm{i}qY_n} \qquad n = 0, \ldots, 6. \tag{16}$$

K_n and Y_n are factors independent of q, and $R_n(q)$ is a rational fraction with L_n poles at $q_{l,n}$, $l = 1, \ldots, L_n$. They are all first-order poles except possibly a second-order pole at $q = \mathrm{i}$.

$$K_0 = \frac{b^{3/2}}{\pi} \qquad K_1 = \frac{4v}{\mathrm{i}\pi} b^{3/2} \qquad K_2 = -K_1 \frac{\mathrm{e}^{-|x|}\mathrm{e}^{-\mathrm{i}x_c(p_c+\mathrm{i}b)}}{b[1+(p_c+\mathrm{i}b)^2]} \tag{17}$$

$$K_3 = -K_1 \frac{\mathrm{e}^{-(|x|-x_c)}}{[b^2+(\mathrm{i}-p_c)^2]} \qquad K_4 = \mathrm{i}K_1 \mathrm{e}^{-|x|} \tag{18}$$

$$K_5 = -K_1 \frac{\mathrm{e}^{-\mathrm{i}x_c(p_c+\mathrm{i}b)}}{\mathrm{i}b[1+(p_c+ib)^2]} \qquad K_6 = -K_1 \frac{\mathrm{e}^{x_c}}{\mathrm{i}[b^2+(\mathrm{i}-p_c)^2]} \tag{19}$$

$$R_0 = \frac{1}{(q-p_c)^2+b^2} \qquad R_1 = \frac{1}{(q-\mathrm{i})^2 C(q)[b^2+(q-p_c)^2]} \tag{20}$$

$$R_2 = \frac{q^2(q+\mathrm{i})}{(q-\mathrm{i})C(q)[q^2-(p_c+\mathrm{i}b)^2]} \qquad R_3 = \frac{q^2}{(q-\mathrm{i})^2 C(q)} \tag{21}$$

$$R_4 = qR_1 \qquad R_5 = R_2/q \qquad R_6 = R_3/q \tag{22}$$

$$Y_0 = x_c - x \qquad Y_1 = x_c - |x| \qquad Y_2 = Y_3 = 0 \qquad Y_4 = x_c \qquad Y_5 = Y_6 = -|x|. \tag{23}$$

The possible pole positions in the seven terms are, in addition to the three roots of the cubic equation $C(q) = 0$, $p = \pm(p_c + \mathrm{i}b)$, $p = p_c - \mathrm{i}b$, and $p = \mathrm{i}$.

The integral in (16) can be performed by completing first the square of the exponent,

$$-\mathrm{i}zt - \mathrm{i}qY_n = -u_n^2 + \mathrm{i}Y_n^2/2t \tag{24}$$

where u_n and f have been introduced for convenience,

$$u_n = (q + Y_n/t)/f \tag{25}$$

$$f = (1-\mathrm{i})\sqrt{1/t}. \tag{26}$$

Let us now expand $R_n(q)$ into partial fractions,

$$R_n(q) = \sum_{l=1}^{L_n} \frac{A_{l,n}}{q - q_{l,n}} + \frac{B_n}{(q - \mathrm{i})^2}. \tag{27}$$

Here $A_{l,n}$ is the residue of $R_n(q)$ at $q_{l,n}$, whereas $B_n = \lim_{q\to \mathrm{i}}(q - \mathrm{i})^2 R_n(q)$ if the double pole appears ($n = 1, 3, 4, 6$), and $B_n = 0$ otherwise ($n = 0, 2, 5$). Explicit expressions for all coefficients are easily obtained from (20)–(22). Once the original integral for $\psi_n(x)$ is decomposed into a sum of integrals for each of the partial fractions, the original contour is deformed along a straight line rotated by $\pi/4$ with respect to the real axis at the saddle point ($u_n = 0$),

$$p_n^{\text{saddle}} = -Y_n/t. \tag{28}$$

This line, D_n, is the steepest descent path of the exponential factor $\mathrm{e}^{-u_n^2}$. Along this path the variable u_n is purely real. Except for $n = 0$, when $x_c - x > 0$, all Y_n are negative, so that the saddle p_n^{saddle} is a positive real momentum. In the deformation process from the original contour Γ to $D_n(t = 0)$, with saddle point $p^{\text{saddle}} = \infty$, the poles at $p_c + \mathrm{i}b$ and i are 'crossed' so their residues have to be added to the integral along D_n, see figure 7. Note that this does not occur for the antiresonance pole when it is in the second quadrant, because the original contour Γ already has a loop around it that disappears in the deformation to $D_n(0)$. The combination of the residue (proportional to an exponential, see (34) and (35) below), and the integral (a w-function) can be expressed, using the definition and symmetry properties of the w-function, see e.g. [13, appendix A], as a single w-function [21]. When t increases D_n moves leftwards, and these two poles are crossed again at certain critical times. But the w-function after the crossing is formally identical to the one before the crossing. Similar considerations apply to the resonance pole and $p_c - \mathrm{i}b$ in the fourth quadrant, so that ψ_n can be finally written as

$$\psi_n(x) = K_n \left\{ \left[\mathrm{i}\pi \sum_l A_{l,n} s_{l,n} w(s_{l,n} u_{l,n}) \right] - 2\mathrm{i}\pi B_n [y_n w(y_n) - \mathrm{i}/\pi^{1/2}]/f \right\} \tag{29}$$

where

$$s_{l,n} = \begin{cases} -1 & \text{antiresonance} \\ \text{sign}[\text{Im}\,(q_{l,n})] & \text{otherwise} \end{cases} \tag{30}$$

$$u_{l,n} = (q_{l,n} + Y_n/t)/f \tag{31}$$

$$y_n = (\mathrm{i} + Y_n/t)/f. \tag{32}$$

(The saddle for ψ_0 when $x_c - x > 0$ moves rightwards from $p = -\infty$ at $t = 0$, but (29) is still valid in this case.) Some of the terms ψ_n can be neglected in special circumstances. The terms with $n = 2, 3, 5, 6$ are only important for small values of $|x_c|$. In 'scattering problems' $|x_c|$ is usually large enough to safely neglect these terms. They would be important in 'decay problems' where the state is initially in the potential region. Moreover, if we are not interested in the potential region, close to the origin $x = 0$, $n = 4$ can also be neglected. In summary, for an asymptotic (large $|x|$) analysis of a packet initially far from the potential centre, $\psi(t) \approx \psi_0 + \psi_1$ is an excellent approximation. In fact, for the reflected wavepacket after the collision ψ_1 is the only important term. In figure 7 a particular configuration of the six poles in R_1 is depicted. These poles have been numbered for later reference: $p_{1,2,3}$ are, as in the previous section, the roots of C, while $p_4 = p_c + \mathrm{i}b$, $p_5 = p_c - \mathrm{i}b$, and $p_6 = \mathrm{i}$. The configuration corresponds to $b < \text{Im}\,(p_1)$ and $p_c > \text{Re}\,(p_1)$. Note that p_4

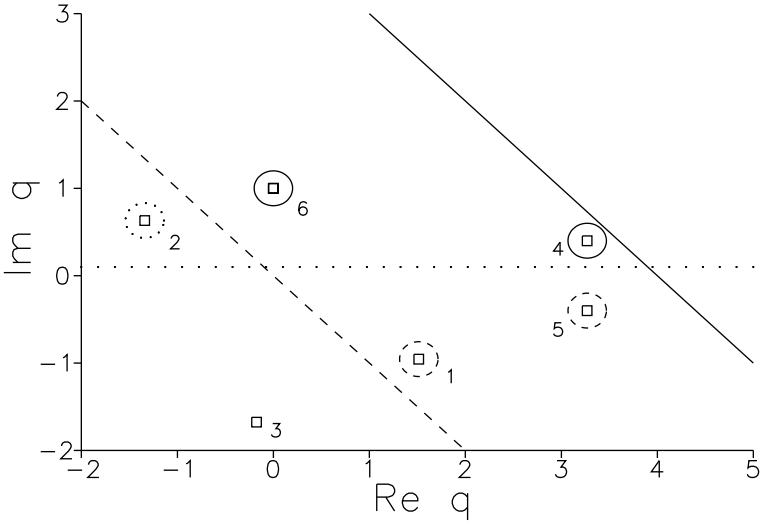

Figure 7. A particular configuration of poles (squares) for ψ_1 in the momentum plane. Also shown is the original integration contour (dotted line), and the deformed contours at short (full line) and long times (broken line). $v = 0.5 - \mathrm{i}$, $p_c = 3.269$, and $b = 0.4$.

and p_5, the 'structural' poles of the initial wavefunction, are also poles for the free motion rational fraction R_0.

Two basic components or approximations for ψ_n are next discussed. At very short times the saddle point of the steepest descent path is far away from all poles on the positive real axis so that the main contribution comes from the large momenta of the saddle itself. The saddle-point contribution to the integral along D_n is obtained by approximating $R_n(u) \approx R_n(0)$ and integrating,

$$\psi_n^{\text{saddle}} = K_n \mathrm{e}^{\mathrm{i}Y_n^2/(2t)} \sqrt{\pi} \left[\frac{B_n}{f y_n^2} - \sum_l \frac{A_{l,n}}{u_{l,n}} \right]. \tag{33}$$

The poles p_4 and p_6 in the upper half-p-plane have been crossed in the deformation from Γ to $D_n(0)$, and the corresponding residues have to be added to the integral along D_n. For the first-order poles the exponential residue contribution is

$$K_n \mathrm{e}^{\mathrm{i}Y_n^2/(2t)} \mathrm{e}^{-u_{l,n}^2} 2\mathrm{i}\pi A_{l,n} \tag{34}$$

and for the second-order pole p_6,

$$\frac{-4\mathrm{i}\pi}{f} y_n K_n B_n \mathrm{e}^{\mathrm{i}Y_n^2/(2t)} \mathrm{e}^{-y_n^2}. \tag{35}$$

The residue from the pole p_4 is particularly important because it grows exponentially with time as the saddle point of D_1 moves leftwards. At the critical time

$$t_4 = -\frac{Y_n}{b + p_c} \tag{36}$$

D_1 crosses p_4 and the residue contribution vanishes. Of course the actual effect of the pole in the total wave is not discontinuous and it is fully taken into account in the corresponding w-function of the exact expression (29), but the crude approximation given by the exponential

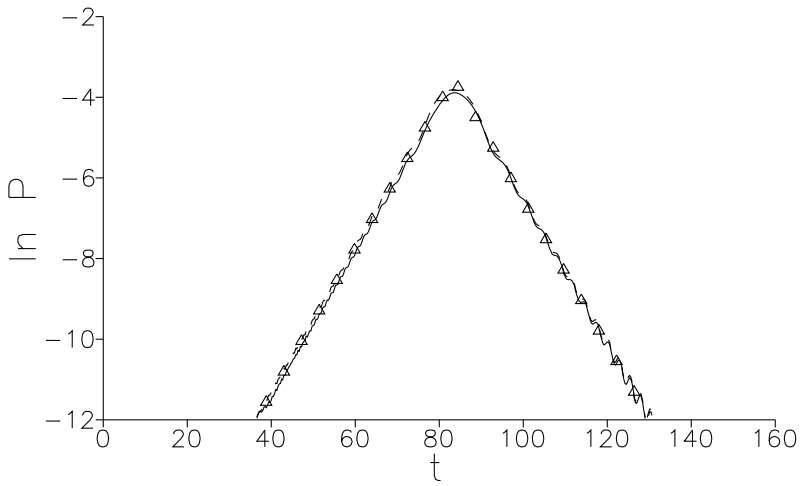

Figure 8. $\ln P$ versus time ($P = |\Psi(x = 100, t)|^2$) for $p_c = 3$, $x_c = -150$, $b = 0.03$, and $v = 5$. $\Psi = \psi$ (full curve); $\Psi = \psi_0$ (broken curve), and $\Psi =$ residue contributions of p_4 and p_5 to ψ_0 (triangles).

gives a very simple, approximate description. Shortly after t_4, the pole $p_5 = p_c - \mathrm{i}b$ in the fourth quadrant is crossed at the critical time

$$t_5 = \frac{Y_n}{b - p_c} \tag{37}$$

(unless $b > p_c$), so that a new residue has to be taken into account. In contrast to the residue from p_4, this one *decreases* exponentially with time because of the pole position in the lower half-plane. The formal contribution is the same as equation (34) but with a minus sign, since the loop around p_5 is clockwise. In this manner the successive effect of the residues from p_4 and p_5 provides the basic 'mechanism' behind the growth and subsequent decay in time of the free wave and the scattered wave. The resonant pole is crossed too so it also contributes with a residue, but for this particular configuration, in which $|\mathrm{Im}\,(p_1)| > b$, it decays faster and can essentially be neglected.

4. Application examples

The time dependence associated with (unitary) resonance scattering or decay of unstable states, in particular the time delays or the exponential decay, has been examined in many works, see e.g. [6–8]. These well known aspects, and other less discussed features of wavepacket propagation can be scrutinized with the present model. For all the applications considered the exact result is provided as well as different approximations. (Further examples of wavepacket scattering and decay making use of the present separable potential model may be found in [9, 12, 13]).

4.1. Resonance scattering: time delay

Figure 8 shows the transmitted probability density at $x = 100$ as a function of time. The initial momentum width is for this figure smaller than the resonance width, $b < |\mathrm{Im}\,(p_1)|$, but the wavepacket has been chosen off-resonance, at $p_c = 3$, in a region where there

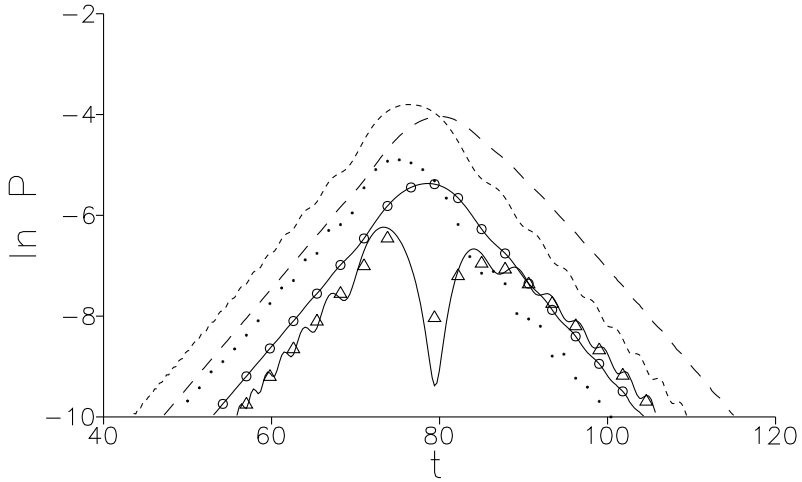

Figure 9. $\ln P$ versus time for $p_c = 3.269$, $x_c = -100$, $b = 0.03$, and $v = 5$. $P = |\Psi(x,t)|^2$. For $\mathrm{Im}\,(v) = 0$, $\Psi = \psi(x = 100)$ (full curve), $\psi_0(x = 100)$ (short broken curve), $\psi_1(x = 100) \approx \psi(x = -100)$ (long broken curve), and $\Psi =$ residue contributions from p_1, p_4 and p_5 at $x = 100$ (triangles). For $\mathrm{Im}\,(v) = -0.25$, $\Psi = \psi(x = 100)$ (dotted curve), $\psi_1(x = 100) \approx \psi(x = -100)$ (full curve with circles).

is essentially full transmission, see figure 1. The full density is basically coincident with the free motion density, which is very well described by the residue contributions from p_4 and p_5 to ψ_0. By contrast, in figure 9 p_c is the real part of the resonance pole. The components $|\psi_0|^2$ and $|\psi_1|^2$ of the probability density are also represented for $x = 100$. In these conditions ψ_s is well approximated by ψ_1. Notice that neither ψ_0 nor ψ_1 dominate. Rather, it is the interference between the two that determines the full wave. A reasonable approximation is obtained by summing the residues of the poles p_1, p_4 and p_5. A minimum is clearly identified in the transmitted wave, which corresponds to reflection caused by the resonance. For negative x there is no significant interference with the free component and $|\psi(x = -100)|^2 \approx |\psi_1(x = -100)|^2 = |\psi_1(x = 100)|^2$. The delay of the scattered or reflected parts and total transmitted density with respect to the free contribution is to be noted. It is related to the positive derivative of the phase of the transmission amplitude for the dominant momentum components [22]. The time delay or advance is one of the signatures of a resonance when the momentum width of the initial packet is smaller than the resonance width. Under these conditions no exponential decay is observed because, as discussed in the previous section, the effect of p_1, with larger imaginary part, decays much faster than that of $p_5 = p_c - \mathrm{i}b$.

4.2. Resonance scattering: exponential decay

The 'exponential decay' of the resonance is best observed when $b > |\mathrm{Im}\,(p_1)|$ in the reflected wavepacket, where ψ_0 is very small and its interference with ψ_s is minimal. This case is illustrated in figure 10. Note that the growth of the probability density is dominated by the wavepacket features, i.e. by the structural pole p_4, while the decay depends on p_1. This asymmetry is of interest, for example, to determine the different times required to 'charge' or 'discharge' mesoscopic structures, such as the well in a double barrier resonant tunnelling diode [23, 24].

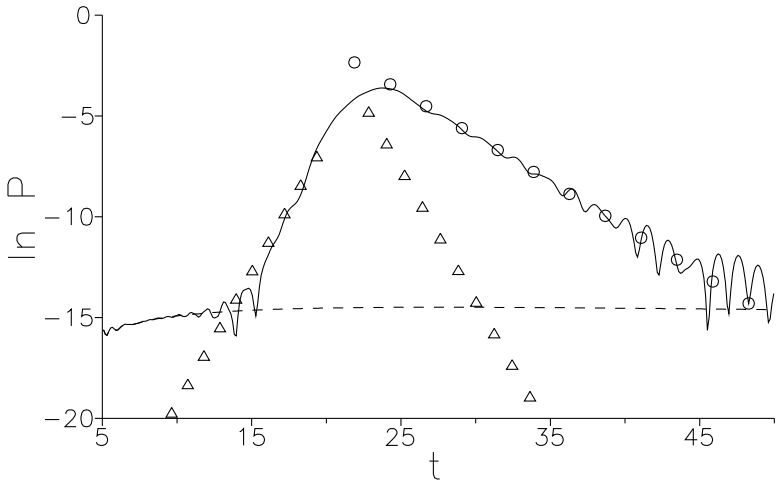

Figure 10. $\ln P$ versus time for $v = 5$, $x_c = -20$, and $p_c = 3.269$. $P = |\Psi(x = -50, t)|^2$. $\Psi = \psi$ (full curve), $\Psi = \psi_0$ (broken curve), $\Psi =$ residue contributions from p_4 and p_5 (triangles), and $\Psi =$ residue contribution from p_1 (circles).

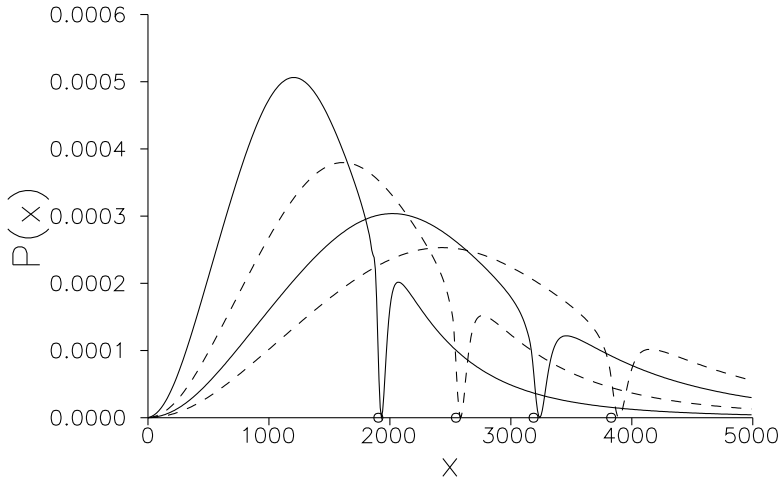

Figure 11. $P(x) = |\psi(x)|^2$ versus x for $t = 600, 800, 1000, 1200$ (full and broken curves alternatively). The positions where D_1 crosses the pole p_1 are indicated with circles. The parameters are $p_c = 2$, $b = 2$, $v = 5$, and $x_c = -20$.

4.3. Effect of the resonance in arbitrary wavepackets

For packets with arbitrary average momentum, but with some overlap with the (real) resonance momentum $p_{\rm res}$, there appears a minimum in the transmitted wavepacket of the probability density at $x_{\rm res}(t)$, see figure 11. This phenomenon was described for the reflected wavepacket (the potentials considered had maximum transmission at resonance) by Bramhall and Casper [25] and by Edgar [26]. The motion of the minimum however was not discussed. This minimum moves with a velocity different from the average velocity of the transmitted packet. Changing the wavepacket parameters, p_c or b, $x_{\rm res}(t)$ remains essentially unaltered. It is therefore a potential dependent (and not state dependent) feature

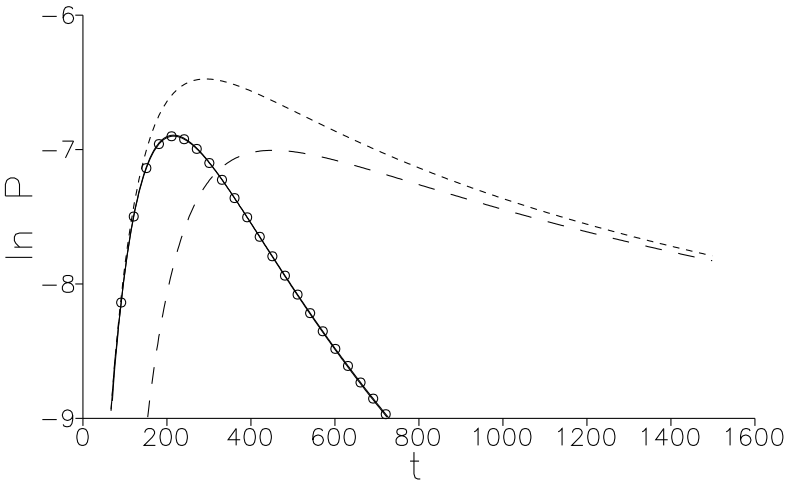

Figure 12. ln P versus time. $v = 5$, $p_c = 0.25$, $b = 1$, and $x_c = -100$. $P = |\Psi(x = 100, t)|^2$. $\Psi = \psi$ (full curve), $\Psi = \psi_0$ (short broken curve), $\Psi = \psi_1$ (long broken curve), and $\Psi = \psi_0^{\text{saddle}} + \psi_1^{\text{saddle}}$ (circles).

associated with the resonance pole. x_{res} is well approximated by the critical position where the steepest descent path D_1 crosses the resonance pole p_1,

$$x_{\text{res}}(t) \approx x_c + [\text{Re}\,(p_1) + \text{Im}\,(p_1)]t. \tag{38}$$

4.4. Low-energy scattering

This potential reflects low-momentum components due to a zero-energy peak in the reflectance. The saddle of the steepest descent path moves from larger momenta (not reflected) at short times to lower momenta (increasingly reflected) at larger times. The consequence of this selective reflection is a seeming advance of the transmitted packet with respect to the free one. An example is shown in figure 12. In this particular case b is quite large and the initial packet has negligible overlap with the resonance region, so that the residues of the poles have very little influence in the final result, which becomes indistinguishable from the saddle approximation $\psi_0^{\text{saddle}} + \psi_1^{\text{saddle}}$ in the scale of the figure. Even though the residues of the poles do not contribute appreciably, the effect of the different singularities can be separated according to their saddle contributions. In figure 12 a good fit with the exact result requires the combined effect of the saddle contributions from p_1, p_3, p_4, and p_6.

4.5. Complex potentials

A complex potential with an imaginary part may be understood in physical terms as an effective interaction for a selected 'channel' [27]. In this context 'absorption' means that there is a passage from the selected channel to other channels. Even if there is no eventual absorption the additional channels may affect the dynamics. As an introductory exploration of the effect of a complex potential in wavepacket dynamics we shall add a negative imaginary part to the potential constant of the separable potential. As discussed in section 2, for large $|\text{Im}\,(v)|$ there is no significant absorption. The important effect in

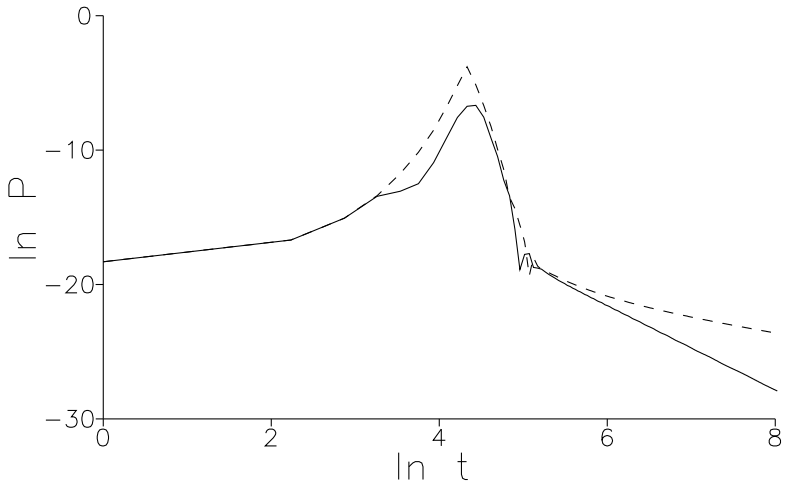

Figure 13. $\ln P$ versus $\ln t$ for $p_c = 3.269$, $x_c = -150$, $b = 0.03$, and $v = 5$. $P = |\Psi(x = 100, t)|^2$. $\Psi = \psi$ (full curve), and $\Psi = \psi_0$ (broken curve).

that limit is the disappearance of the resonance peak (figure 1) and as a consequence all related features of wavepacket resonant scattering. For small values of Im (v) the absorptive potential has two significant effects: absorption, and an asymmetrical time advance/delay for the transmitted/reflected packet with respect to free motion when p_c is tuned with the resonance, see figure 9, and the explanation provided in section 2.

4.6. Asymptotic behaviour at very large times

For large times the saddle points of the integration steepest descent paths D_n are very close to the origin $q = 0$. Moreover the exponentials $e^{-u_n^2}$ become very narrow Gaussians in the complex momentum plane. Thus an asymptotic formulae for the long-time behaviour can be derived by expanding in the integrands of ψ_0 and ψ_s the factors I_0 and I_s that multiply these exponentials around the origin and retaining the first terms, see (14), (15),

$$\langle x|\psi\rangle \sim \frac{(1-\mathrm{i})}{4\pi^{1/2}}\left(\frac{1}{t}\right)^{3/2}\frac{\mathrm{d}^2}{\mathrm{d}q^2}(I_0 + I_s)_{q=0} \tag{39}$$

so that the probability density decays asymptotically as t^{-3}, see figure 13. This is in contrast to the dependence t^{-1} of free motion, where there is no scattering contribution to cancel the zeroth-order term. The asymptotic limit and the integration over x commute because the asymptotic series holds uniformly so that the series can be integrated term by term [28]. This means that the probability to remain in a certain region ('non escape' probability) has also the asymptotic dependence t^{-3} as $t \to \infty$ [11, 29]. This aspect has been controversial and opposite claims have made in [30].

4.7. Asymptotic behaviour at very short times

The probability density when the ratio x/t is large is now examined. In this case all poles are far from the steepest descent paths D_n, and the saddle approximation (33) can be used. Moreover, p_1^{saddle} is very large so the residues $A_{l,1}$ are very small and the contribution from ψ_1^{saddle} can be neglected with respect to the contribution from ψ_0^{saddle}. The consequence

is that the 'tip' of the wavepacket is the same with or without interaction potential. This should be expected since the very large-momentum components which determine the wave behaviour in this regime are hardly affected by the potential. In summary, the asymptotic expression for $\psi(x, y)$ is obtained taking into account that $\psi \sim \psi_0 \sim \psi_0^{\text{saddle}}$,

$$|\psi(x)|^2 \sim \frac{2b^3}{\pi t} \frac{1}{\{[p_c + (x_c - x)/t]^2 + b^2\}^2} \sim \frac{2b^3 t^3}{\pi (x_c - x)^4}. \tag{40}$$

5. Conclusions

The time-dependent collision of an initial Lorentzian-like state with a separable potential model has been solved analytically in terms of w-functions. Besides the exact solution, simple approximations based on the main contributions from critical points have been provided to gain intuitive insight into the various phenomena discussed: different aspects of resonance scattering, low energy scattering, complex potential scattering, or short- and long-time behaviour. We have described in particular an interesting asymmetry between the delays of the transmitted and reflected wavepackets for complex potentials. This work has dealt with scattering states with *in* and *out* asymtotes. A complementary study on 'decay' problems for the same potential may be found in [12, 13]. For this model there is a single resonance, but multiple resonance systems, such as a double delta barrier [31], can be studied with the same techniques used here. The 'shutter problem' with a square barrier has been already treated in this fashion [22].

Acknowledgments

We are grateful to R F Snider for many discussions. This work was supported by Gobierno Autónomo de Canarias, grant PI2 /95, and by Ministerio de Educación y Cultura, grant PB97-1482. JPP acknowledges an FPI fellowship (PB 93-0578) from Ministerio de Educación y Cultura.

References

[1] Elberfeld W and Kleber M 1988 *Am. J. Phys.* **56** 154
[2] Muga J G and Brouard S 1992 *Phys. Rev.* A **46** 6075
[3] Snider R F 1988 *J. Chem. Phys.* **88** 6438
[4] Muga J G and Snider R F 1990 *Can. J. Phys.* **68** 394
[5] Muga J G and Snider R F 1990 *Can. J. Phys.* **68** 403
[6] Fonda L and Ghirardi G C 1970 *Nuovo Cimento* A **67** 257
[7] Fonda L, Ghirardi G C and Rimini A 1978 *Rep. Prog. Phys.* **41** 587
[8] Misra B and Sudarshan E C G 1977 *J. Math. Phys.* **18** 756
[9] Hammerich A D, Muga J G and Kosloff R 1989 *Isr. J. Chem.* **29** 461
[10] Snider R F and Muga J G 1993 *Can. J. Chem.* **72** 152
[11] Muga J G, Delgado V and Snider R F 1995 *Phys. Rev.* B **52** 16 381
[12] Muga J G, Wei G W and Snider R F 1996 *Europhys. Lett.* **35** 247
[13] Muga J G, Wei G W and Snider R F 1996 *Ann. Phys., NY* **252** 336
[14] Ghirardi G C and Rimini A 1964 *J. Math. Phys.* **5** 722
[15] Newton R G 1980 *J. Math. Phys.* **21** 493
[16] Kamal A N 1984 *Am. J. Phys.* **52** 46
[17] Cassing W, Stingl M and Weiguny A 1982 *Phys. Rev.* C **26** 22
[18] Sassoli de Bianchi M 1994 *J. Math. Phys.* **35** 2719
[19] Joffily S 1973 *Nucl. Phys.* A **215** 301

[20] Similar advances occur, but at zero energy and for real attractive potentials, in the presence of loosely bound states, see van Dijk W and Kiers K A 1991 *Am. J. Phys.* **60** 520
[21] Abramowitz M and Stegun I A 1972 *Handbook of Mathematical Functions* (New York: Dover)
[22] Brouard S and Muga J G 1996 *Phys. Rev.* A **54** 3055
[23] Stovneng J A and Hauge E H 1991 *Phys. Rev.* B **44** 13 582
[24] Walker D B, Glytsis E N and Gaylord T K 1994 *J. Appl. Phys.* **75** 5415
[25] Bramhall M H and Casper B M 1970 *Am. J. Phys.* **38** 1136
[26] Edgar A 1995 *Am. J. Phys.* **63** 136
[27] Taylor J R 1972 *Scattering Theory* (New York: Wiley) pp 383–8
[28] Bleistein N and Handelsman R A 1986 *Asymptotic Expansions of Integrals* (New York: Dover) pp 29–30
[29] Cavalcanti R M 1998 *Phys. Rev. Lett.* **80** 4353
[30] García Calderón G, Mateos J L and Moshinsky M 1995 *Phys. Rev. Lett.* **74** 337
García Calderón G, Mateos J L and Moshinsky M 1996 *Ann. Phys.* **249** 430
García Calderón G, Mateos J L and Moshinsky M 1998 *Phys. Rev. Lett.* **80** 4354
[31] Hammer C L, Weber T A and Zidell V S 1977 *Am. J. Phys.* **45** 933